

# 23

## Whirls and vortices

Whirls and vortices are common features of real fluids. Stirring the coffee, you create a circulating motion, a whirl that dies out after some time when you stop stirring. A fast spinning vortex may be created at the drain of a bathtub when it is emptied, and it may remain quasi-stable as long as there is enough water in the tub. Normally, whirls and vortices are invisible far away from free boundaries, but in the bathtub the drain vortex is made visible by soap remains clouding the water and the depression it creates at the surface. It may even become audible, because water falling through the drain sucks air down from the surface.

In the atmosphere above heated ground, whirls and vortices arise all the time. Mostly they are small and invisible, but sometimes they pick up dust and debris and appear as dust devils. Larger dust devils, in some countries called sky-pumps, are known to pick up haystacks and scatter them, or to throw tables around in sidewalk cafes. When the heat-driven air vortices grow really big and nasty, they may become tornadoes. The force powering heat-driven vortices is the same as the force that maintains a bathtub vortex, namely gravity. In the bathtub the vortex is sustained by gravity's work on the water falling through the drain, and in the atmosphere by its work on updrafts caused by the buoyancy of bubbles of hot air.

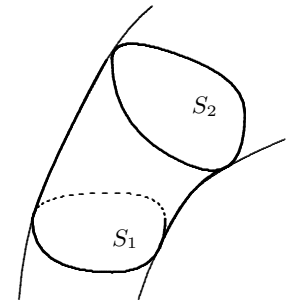
Vortices are also found in the wakes of moving objects. From the tips of the wings of aircraft there will always be invisible trailing vortices (to be discussed in chapter 26). Large passenger aircraft taking off or landing create strong and fairly stable vortices, capable of overturning smaller planes following after. "Beware of vortex" is a common warning issued by flight controllers to small aircraft during takeoff and approach to landing.

The chapter opens with the strong theorems due to Stokes, Kelvin and Helmholtz that give us insight into vortex dynamics in nearly ideal fluids, but the general focus is on explicit models for non-singular vortices. Extensive treatment of vortex structure and dynamics may be found in [44, 45].

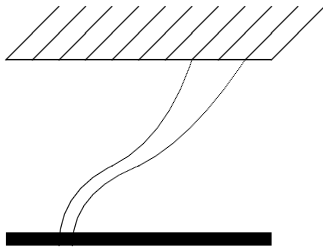
## 23.1 Basic vortex dynamics

Vortex lines were defined (page 283) to be curves that everywhere follow the instantaneous vorticity field,  $\boldsymbol{\omega} = \nabla \times \mathbf{v}$ . Like streamlines, vortex lines cannot cross each other, and since the vorticity field is divergence-free,  $\nabla \cdot \boldsymbol{\omega} = 0$ , vortex lines cannot emerge from anywhere, but must form closed curves, or curves coming from and going to the boundaries of the flow (or to spatial infinity). Vortex dynamics is quite complicated [44, 45], and we shall here only present a few general results, mainly due to Helmholtz.

Hermann von Helmholtz  
(1821–94). *Austrian poly-  
histor.*



The flux of vorticity is the same in every cross section of a vortex tube.



A tornado funnel is a vortex connecting the ground and the thundercloud. Typically, the cloud moves and drags the top of the tornado along.

### Vortex tubes

The set of vortex lines that go through the points of a closed curve at a given time  $t$  form together a *vortex tube* that may curve and bend in space. We shall now prove, that whatever shape it takes, it will nevertheless have the same total flux of vorticity through every cross section. To prove this we just use Gauss' theorem on the closed surface formed by a stretch of vortex tube between two cross sections,  $S_1$  and  $S_2$ . Since the divergence of the vorticity field vanishes,  $\nabla \cdot \boldsymbol{\omega} = 0$ , the closed surface integral over this stretch of tube must vanish,

$$\oint_S \boldsymbol{\omega} \cdot d\mathbf{S} = \int_{S_2} \boldsymbol{\omega} \cdot d\mathbf{S} - \int_{S_1} \boldsymbol{\omega} \cdot d\mathbf{S} = 0. \quad (23-1)$$

The sides of the tube do not contribute to the integral, because the surface elements are orthogonal to the vortex lines, *i.e.* to the vorticity field.

The common flux through any cross section of a vortex tube is called the *strength* of the tube, and by Stokes theorem (15-67) this flux equals the circulation around the tube. Most real vortices will have a central vortex tube, called the *core* of the vortex, containing almost all of the vorticity, with the flow being nearly irrotational outside. The spindle-driven vortex (18-66), discussed on page 376, has precisely this structure with the spindle itself playing the role of the core and a perfectly irrotational flow  $v_\phi \sim 1/r$  outside. The remaining sections in this chapter mainly turn around what happens when the external spindle is replaced by a fluid core, making it an all fluid vortex.

### Vortex filaments

Kelvin's circulation theorem (15-69) states that in an *inviscid* fluid a comoving vortex tube never changes its strength, independently of how it is blown around by the ambient flow. Since it cannot disappear, an inviscid vortex acquires an identity of its own. It may connect to the boundaries (possibly at infinity), but often it will take the form of a closed loop, like a smoke ring drifting around in space.

In the extreme and singular limit, where the vortex core becomes infinitely thin and its vorticity field infinitely high while the strength remains finite, it is called a *vortex filament*. A vortex filament is entirely characterized by its strength

and the curve that describes the whereabouts of the core. In the simplest case, the *line vortex*, the core is a straight line and the velocity field is the same as for the spindle vortex (18-66) in the limit of the spindle having vanishing radius and infinite angular velocity,

$$\boxed{v_\phi = \frac{C}{r}}. \tag{23-2}$$

The circulation,  $\Gamma = 2\pi r v_\phi = 2\pi C$ , is independent of  $r$ , demonstrating through Stokes' theorem that the field is free of vorticity. The vortex core is here an infinitely thin straight line of vorticity connected to spatial infinity, but as discussed above it may move around, bend and twist without ever losing a turn, provided that there is no viscosity. In the following section we shall learn that viscosity will make the vortex core expand and eventually cause the vortex to disappear, but if the length and time scales are right, a real vortex may in fact behave as a filament.

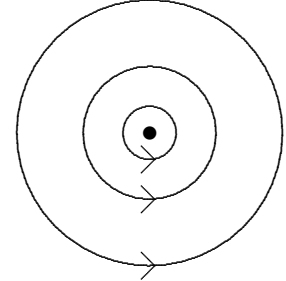
### Interactions between line vortices

Vortices are not always loners like the bathtub vortex or the tornado, but may interact with other vortices or even with different parts of themselves, giving rise to a number of interesting and sometimes counterintuitive phenomena. In truly ideal fluid, the only possible interaction is the advection of one vortex in the flow created by the others. Each vortex is simply blown around in the winds created by all the other vortices.

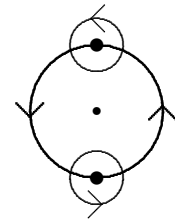
A pair of parallel line vortices with the same strength  $C$  and a distance  $d$  between the cores, will blow each other in opposite directions. For symmetry reasons, the two vortex cores will dance around each other on a circle of radius  $r = d/2$ . If  $\Omega$  is the angular velocity in this dance, the velocity difference between the cores must obey  $2\Omega r = C/r$ , or  $\Omega = C/d^2$ . A pair of opposite strength,  $C$  and  $-C$ , will blow each other in the same direction, and for symmetry reasons move in unison through the fluid with a common velocity  $C/d$ . For them to remain in place, an opposite ambient wind of strength  $-C/d$  is needed.

An isolated ring vortex interacts in the same way with itself and propagates, somewhat counterintuitively, through the fluid with constant speed in the same direction as the flow inside the ring. Before the present virtual ban on smoking, fathers would habitually impress their children by creating beautiful rings from cigar or cigarette smoke. The ring was formed by sharply blowing smoke-laden air through a circular opening made by the lips. The initial burst of air would carry the ring forward, but the ring could be observed to continue forwards far beyond the range of the initial burst, to the delight of the children and — with our present knowledge — also to their detriment!

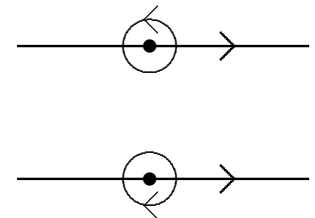
In the wake of a moving cylinder a slower moving regular pattern of vortices, called the *von Kármán vortex street*, will be formed at Reynolds numbers below the onset of turbulence (see for example [40, ch. 5] or [16, p. 155]) for a more quantitative discussion of this phenomenon).



*Irrotational flow outside the core of a line vortex. The circulation is the same around any flow line.*



*Two parallel line vortices of equal strength cause the cores of each other to move on a common circle. More vortex filaments may participate in the dance.*



*Two line vortices of equal but opposite strength blow each other in the same direction with the same speed, here towards the right. The same picture could also describe a cross section through the center of a smoke ring.*

## 23.2 Free cylindrical vortices

The line vortex (23-2) is singular, carrying infinite vorticity in its infinitely thin core. This of course unphysical; any real vortex in a fluid with finite viscosity must have finite vorticity everywhere and a finite core radius.

In this section we shall study vortices that are closely related to the singular line vortices. These vortices are *free* of all external driving forces, such as gravity, and the azimuthal flow  $v_\phi(r)$  is assumed to be the only non-vanishing component of the velocity field. We shall see that such vortices are necessarily unsteady and decay away because of viscous dissipation of their kinetic energy. In the following section we take up the problem of how to create steady vortices in the presence of viscosity by feeding energy and angular momentum to them through secondary flow.

### The Rankine vortex

The spindle-driven vortex discussed on page 376 was powered by a rotating cylindrical spindle, which delivered the work necessary to overcome viscous friction in the fluid. Although the flow pattern (18-66) did not depend explicitly on the viscosity of the fluid, a finite viscosity was nevertheless necessary for the spindle to be able to “crank up” the vortex, starting from fluid at rest.

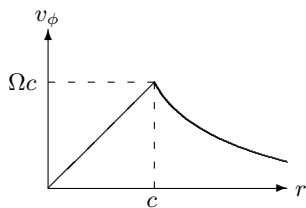
In a truly inviscid fluid, we would not be able to crank up the vortex, but once it had somehow been established there would be no viscous losses and the vortex would keep spinning forever. The solid spindle could then with impunity be replaced by a *core* made from the same fluid as the vortex and rotating as a solid body with the same angular velocity as the spindle. The *Rankine vortex* with core radius  $c$  is constructed in precisely this way,

$$v_\phi = \begin{cases} \Omega r & 0 \leq r \leq c \\ \frac{\Omega c^2}{r} & c \leq r < \infty \end{cases}. \quad (23-3)$$

Its vorticity vanishes outside the core and is constant inside (see problem 18.27). Since there is no secondary flow, the general theory of purely circulating flow developed in section 18.9 on page 371 must be valid. One notices the peculiarity that both the inner and the outer Rankine vortex fields belong to the general class of solutions (18-53), although the complete Rankine field does not.

Although the Rankine velocity field is continuous everywhere, it has a cusp at the core boundary. If the viscosity does not vanish, this cusp will produce a jump in shear stress (18-57) from  $\sigma_{\phi r} = 0$  everywhere inside the core to  $\sigma_{\phi r} = -2\eta\Omega$  just outside. Such a jump is physically unacceptable because it violates Newton's third law which requires continuity of the stress vector across any boundary. The Rankine vortex is strictly speaking only meaningful for a truly inviscid fluid.

William John Macquorne Rankine (1820–72). *Scottish engineer and physicist.*



*Sketch of the velocity field for the Rankine vortex. In a viscous fluid the cusp at the core boundary  $r = c$  indicates a discontinuity in shear stress which is physically unacceptable.*

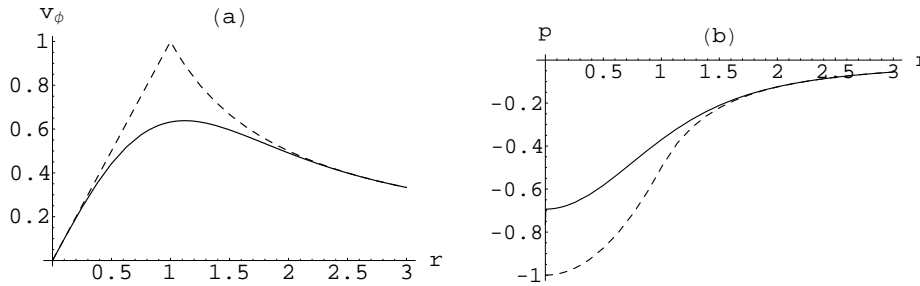


Figure 23.1: *The interpolating vortex (fully drawn) and the Rankine vortex (dashed) for  $c = \Omega = \rho_0 = 1$  (a) The velocity field. (b) The pressure field, which is somewhat shallower than for the Rankine vortex.*

### Interpolating vortex

When two partial solutions do not match, it is sometimes possible to find a smooth interpolating function which coincides with the partial solutions in most of their respective domains<sup>1</sup>. For the Rankine vortex we may take

$$v_\phi = \frac{\Omega c^2}{r} \left( 1 - \exp\left(-\frac{r^2}{c^2}\right) \right). \quad (23-4)$$

This expression approaches the Rankine solution for both  $r \ll c$  and for  $r \gg c$ , but the shear stress is now continuous everywhere and the problem with Newton's third law has disappeared. The shape of the vortex is shown in fig. 23.1a together with the Rankine vortex (dashed).

In the absence of gravity, the pressure  $p = p(r)$  can only depend on  $r$ , and the radial pressure gradient must deliver the centripetal force necessary for the circular fluid motion,

$$\frac{dp}{dr} = \rho_0 \frac{v_\phi^2}{r} \quad (23-5)$$

Integrating this equation with the interpolating vortex (23-4), and normalizing the pressure to vanish at spatial infinity, we get the picture in fig. 23.1b. The pressure is lower at the center compared to infinity, and for a liquid vortex in gravity this would create a central depression in the open surface of the same shape (see section 23.5).

### Diffusive spin-down of a free vortex

The resolution of the stress problem comes at a price, because the interpolating vortex cannot be stable on its own in a viscous fluid. The shear stress will cause dissipation of kinetic energy everywhere in the fluid and make the vortex spin down. The largest shear stress is found just outside the core and will primarily

<sup>1</sup>Planck's discovery of the spectrum of blackbody radiation in the year 1900 is by far the most famous such interpolation ever made.

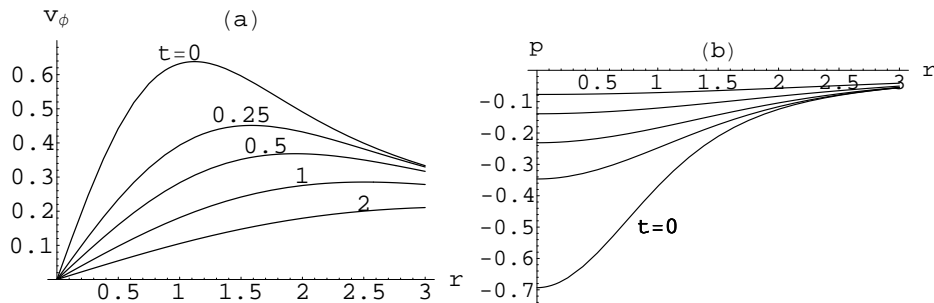


Figure 23.2: Time evolution of the Oseen-Lamb vortex (23-7) for  $c = \Omega = \nu = 1$  at selected times. The core grows larger with time while the central angular velocity (i.e. the slope at  $r = 0$ ) becomes smaller. (a) The azimuthal field. (b) The pressure distribution.

slow down the core's rotation while expanding its radius. The flow at greater distances from the core is left undisturbed until the expanding core reaches it.

Assuming that the azimuthal velocity field retains its purely cylindrical form  $v_\phi(r, t)$  at all times, the time-dependent Navier-Stokes equation for this field becomes in cylindrical coordinates,

$$\boxed{\frac{\partial v_\phi}{\partial t} = \nu \frac{\partial}{\partial r} \left( \frac{1}{r} \frac{\partial (r v_\phi)}{\partial r} \right)}. \quad (23-6)$$

This equation is quite analogous to the momentum diffusion equation (??), except for the extra complication of cylindrical coordinates. Given any initial field  $v_\phi(r, 0)$ , this equation will always yield a solution.

One may by insertion directly verify that the solution which for  $t = 0$  equals the interpolating vortex (23-4) is,

$$v_\phi(r, t) = \frac{\Omega c^2}{r} \left( 1 - \exp \left( -\frac{r^2}{c^2 + 4\nu t} \right) \right). \quad (23-7)$$

It is called the *Oseen-Lamb vortex*. It should be mentioned that there are many other exact solutions to (23-6) (see problems 23.8 and 23.9).

The time evolution of the vortex is plotted in fig. 23.2a. The core radius,  $c(t) = \sqrt{c^2 + 4\nu t}$ , grows with time while the angular velocity of the core,  $\Omega(t) = \Omega c^2 / (c^2 + 4\nu t)$  decreases. The time it takes for the vortex to “forget” its original core size is  $t \gtrsim c^2 / 4\nu$ , and the core overtakes any point  $r$ , well outside the original core, in a time  $t \gtrsim r^2 / 4\nu$ . These times are recognized as typical momentum diffusion time scales (see page 337). In this case the quantity that diffuses is actually angular momentum.

**Example 23.2.1:** A water vortex with core radius  $c = 3$  cm has a viscous core spin-down time of  $c^2 / 4\nu = 260$  s, i.e. a little more than 4 minutes. This is surprisingly large, but it should be remembered that the estimate is only valid for laminar flow. Most real-life bathtub vortices don't last that long (unless they are fed by inflow), because they spin so rapidly that their energy is quickly lost to turbulence.

### 23.3 Steady vortex sustained by secondary flow

Intuitively, it seems as if the natural tendency for the free vortex core to expand under the influence of viscosity could be counteracted by a sufficiently strong steady radial inflow,  $v_r$ . Since the radial inflow of fluid cannot accumulate at the center of the vortex, there must necessarily also be a steady axial outflow,  $v_z$ . We shall again restrict the analysis to cylindrical vortices, in which the primary azimuthal flow only depends on the radial coordinate  $r$ , *i.e.*  $v_\phi = v_\phi(r)$ . More general steady cylindrical vortices, in which the primary azimuthal flow  $v_\phi$  also depends on  $z$ , are also possible, for example the forced flow between two parallel plates rotating with different angular velocities.

The basic mechanism that shapes a steady vortex in the presence of radial inflow, is conservation of angular momentum. The angular momentum of a fluid particle of constant mass  $dM$  is  $d\mathcal{L}_z = rv_\phi dM$ . If the radial inflow is so strong that it overwhelms the loss of angular momentum due to viscous torque acting on the particle, its angular momentum  $d\mathcal{L}_z$  must be constant. This implies that the specific angular momentum,  $d\mathcal{L}_z/dM = rv_\phi$ , must be constant, and the vortex acquires the characteristic shape of a line vortex,  $v_\phi \approx C/r$ , far from the core.

#### Vortex equations

In the presence of secondary flow, the azimuthal equation for steady flow contains advective terms on the left hand side. Under the assumption that  $v_\phi = v_\phi(r)$  only depends on  $r$ , the equation becomes (see also problem 23.5)

$$\boxed{\frac{v_r}{r} \frac{d(rv_\phi)}{dr} = \nu \frac{d}{dr} \left( \frac{1}{r} \frac{d(rv_\phi)}{dr} \right)} . \quad (23-8)$$

It follows from this equation that the radial flow likewise can only depend on  $r$ , *i.e.*  $v_r = v_r(r)$ .

The relation between radial and axial flow is given by the equation of continuity, which in cylindrical coordinates takes the form

$$\frac{1}{r} \frac{d(rv_r)}{dr} + \frac{\partial v_z}{\partial z} = 0 . \quad (23-9)$$

Solving for  $v_z$  we obtain,

$$\boxed{v_z(r, z) = w(r) - \frac{z}{r} \frac{d(rv_r(r))}{dr}} , \quad (23-10)$$

where  $w(r)$  is an arbitrary function that specifies the axial flow at  $z = 0$ . The second term represents the accumulated radial inflow.

### Radial Reynolds number

Since  $v_\phi$  occurs on both sides of (23-8), the ratio of the advective to viscous terms is independent of  $v_\phi$ . Therefore, the quantity which characterizes the solutions is the radial Reynolds number

$$\text{Re}_r = \frac{r |v_r|}{\nu} . \quad (23-11)$$

When  $\text{Re}_r \gg 1$ , the right hand side of (23-8) can be disregarded, and the solutions must satisfy  $d(rv_\phi)/dr \approx 0$ , in other words  $v_\phi \approx C/r$ . This confirms the more intuitive analysis concerning angular momentum and gives a meaning to the phrase “sufficiently strong radial inflow”.

In contrast, when  $\text{Re}_r \ll 1$ , the left hand side of (23-8) can be disregarded. This typically happens for  $r \rightarrow 0$ , and the only solution to the resulting equation which is regular at  $r = 0$  is  $v_\phi \approx \Omega r$ . So even if the inflow is strong enough for large  $r$ , it will never be strong enough for sufficiently small  $r$ . Close to the center of the vortex, viscous forces will come to dominate and make the core rotate as a solid body with angular velocity  $\Omega$ . The core radius  $c$  may be estimated by equating the long and short distance expressions,  $\Omega r \approx C/r$ , leading to,

$$c \approx \sqrt{\frac{C}{\Omega}} . \quad (23-12)$$

Any flow-sustained steady vortex will thus in its gross structure resemble the interpolating Rankine vortex (see fig. 23.1).

### The Burgers vortex

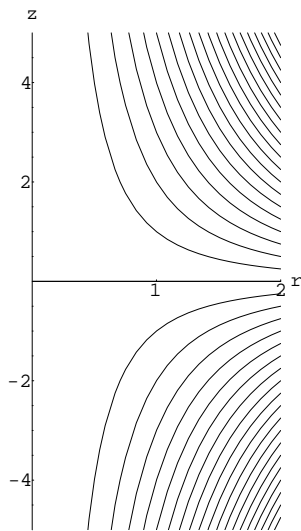
From the vortex equations one may find the inflow necessary to maintain *any* azimuthal flow  $v_\phi(r)$ . Inserting your favorite vortex  $v_\phi(r)$  into (23-8), you immediately find the radial flow  $v_r(r)$ , and afterwards you can calculate the axial flow  $v_z$  from (23-10), given your favorite choice of  $w(r)$ . Thus, the complete flow field which maintains the interpolating vortex (23-4) is (for  $w = 0$ ),

$$v_\phi = \frac{\Omega c^2}{r} \left( 1 - \exp\left(-\frac{r^2}{c^2}\right) \right) , \quad (23-13a)$$

$$v_r = -\frac{2\nu}{c^2} r , \quad (23-13b)$$

$$v_z = \frac{4\nu}{c^2} z . \quad (23-13c)$$

It is called the *Burgers vortex* and is in fact an exact solution to the full set of steady-flow Navier-Stokes equations (see problem 23.5). The scale of the secondary flow is set by the inverse of the viscous core expansion time,  $4\nu/c^2$ , but that is not particularly surprising, since the purpose of the secondary flow is precisely to counteract core expansion. For  $\nu \rightarrow 0$ , the secondary flow disappears and the Burgers vortex becomes identical to the interpolating vortex, as one would expect.



*Streamlines for secondary flow in the Burgers vortex. The pattern is mirror symmetric in  $z = 0$ . The actual streamlines are spirals that circle around the center of the vortex while contracting and moving upwards or downwards along the axis.*



### Vortex with singular axial jet

In the Burgers vortex, the axial flow is independent of  $r$ , and that makes very different from naturally born vortices, such as the bathtub vortex, where the axial downflow must converge upon a small drain, or the tornado where the axial upflow appears to take place inside a narrow funnel. Here we shall consider the extreme case of a vortex with a localized *axial jet*. The model is a generalization of the line vortex (23-2), and could be taken as a primitive model of a gas vortex, *i.e.* a “tornado”.

By assumption, the axial flow vanishes outside the singular jet, or  $v_z = 0$  for  $r > 0$ . It then follows from the explicit expression for the axial flow (23-10), that both  $w(r) = 0$  and  $d(rv_r)/dr = 0$ , implying that the radial flow must be of the form,

$$v_r = -\frac{q}{r} . \quad (23-14)$$

Here  $q$  is a positive constant that sets the scale of the inflow. The total volume of fluid that flows radially in through the vortex over an axial length  $L$  is independent of  $r$ ,  $Q = -2\pi r L v_r = 2\pi q L$ . Mass conservation tells us that this must equal the amount of fluid that is carried away by the singular axial jet.

It may be verified by insertion that with this radial inflow the most general solution to (23-8) is,

$$v_\phi = \frac{C}{r} + A r^{1-q/\nu} , \quad (23-15)$$

where  $C$  and  $A$  are constants. The second term decays faster than the first at infinity for  $\text{Re}_r = q/\nu > 2$ , and this confirms that the radial inflow must be larger than a certain minimum for the azimuthal flow to approach that of a line vortex at large distances.

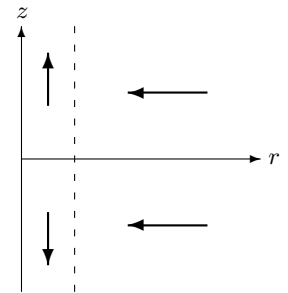
### Extended axial jet

In a more realistic “tornado” model, the axial jet has a finite radius  $r = a$ . It is tempting to model the flow inside the axial jet with Burgers vortex (23-13) and outside with the singular solution (23-15), and afterwards match the two solutions at  $r = a$ , but that leaves a rather unphysical jump in the axial flow at this place. It is for this reason better to choose a softer radial flow, interpolating smoothly between the singular jet and the Burgers vortex, for example,

$$v_r = -\frac{q}{r} \left( 1 - e^{-r^2/a^2} \right) . \quad (23-16)$$

The axial flow now follows from (23-10),

$$v_z = z \frac{2q}{a^2} \exp\left(-\frac{r^2}{a^2}\right) , \quad (23-17)$$



Sketch of the general structure of the secondary flow pattern in a vortex with a soft axial jet.

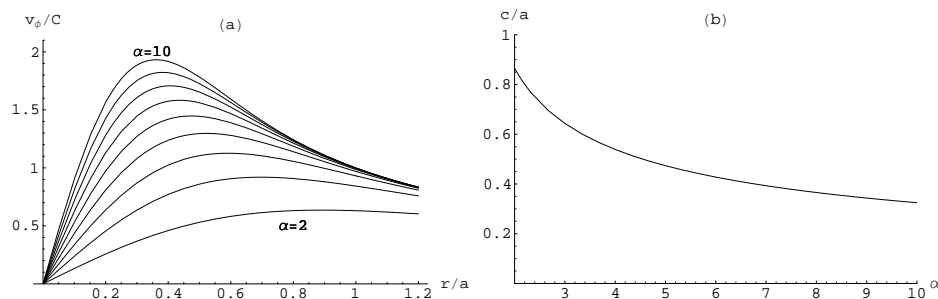


Figure 23.3: **(a)** Azimuthal flow in a vortex with non-singular axial jet (23-16) plotted for various values of the dimensionless inflow scale  $\alpha = q/2\nu$ . **(b)** The core radius  $c = \sqrt{C/\Omega}$  corresponds roughly to the top in  $v_\phi$  and shrinks as the inflow scale grows.

where we have chosen  $w = 0$ . Clearly, this expression vanishes rapidly for  $r > a$ , as it should.

Although the vortex equation (23-8) may be integrated numerically by quadrature (see problem 23.13), it is simpler to solve it numerically as a second order differential equation. The result normalized by  $a$  and  $C$  is shown in fig. 23.3a for a selection of values of  $\alpha = q/2\nu$ . In fig. 23.3b, the core radius (23-12) is plotted as a function of  $\alpha$ .

### 23.4 Advective spin-up of a cylindrical vortex

It is a common observation that a vortex can be “spun” up by draining fluid from its central region at a steady rate. Suppose the drain is constructed such that a steady radial inflow  $v_r(r)$  is established. If the inflow is sufficiently large, the advective terms will dominate over the viscous terms far from the core,  $r \gg c$ , so that the vortex in this region must obey the time-dependent azimuthal equation

$$\frac{\partial v_\phi}{\partial t} + \frac{v_r}{r} \frac{\partial(rv_\phi)}{\partial r} = 0. \quad (23-18)$$

To solve this equation, we first solve the differential equation  $dr/d\tau = -v_r(r)$ . The solution is,

$$\tau(r) = - \int \frac{dr}{v_r(r)}. \quad (23-19)$$

Apart from an undetermined constant, this may be interpreted as the time it takes the fluid to move to the center through the radial distance  $r$ . Since  $v_r < 0$ , this function grows monotonically with  $r$ . If, for example, the radial flow is that of a singular axial jet (23-14), we have  $\tau = r^2/2q$ .

Using this variable, the advective equation (23-18) takes the form

$$\frac{\partial(rv_\phi)}{\partial t} = \frac{\partial(rv_\phi)}{\partial \tau}.$$

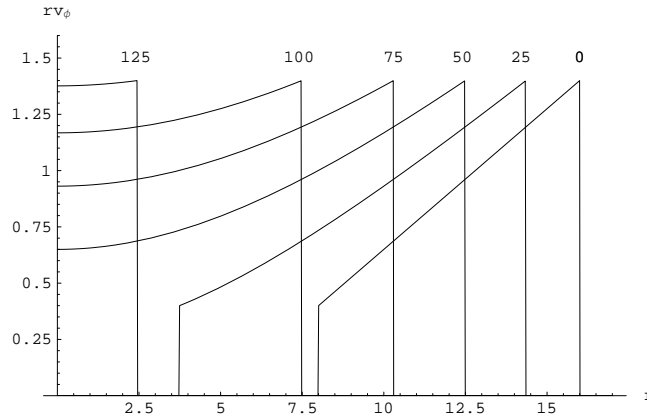


Figure 23.4: “Movie” of advective spin-up of a vortex with a singular axial jet. The specific angular momentum  $rv_\phi$  is plotted as a function of radial distance for selected times (shown above the curves), starting with  $t = 0$ . The initial shape is progressively flattened and eventually, for  $t = 128$ , has completely gone down the drain at the left.

The most general solution is  $rv_\phi = f(t + \tau)$  where  $f(\cdot)$  is an arbitrary function. In the usual variables we have

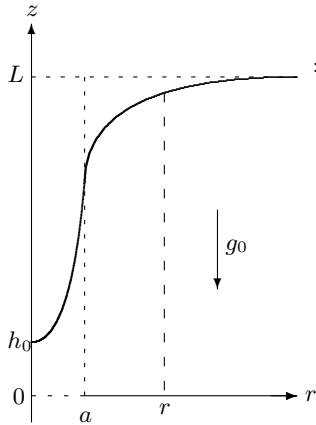
$$v_\phi(r, t) = \frac{f(t + \tau(r))}{r}. \quad (23-20)$$

The shape of  $f$  may be determined from the initial azimuthal field at  $t = 0$ , which satisfies  $f(\tau(r)) = rv_\phi(r, 0)$ .

We are now in position to discuss the advective spin-up of the vortex. Since  $\tau(r)$  grows monotonically with  $r$ , it follows that inside any given radial distance,  $c \ll r < R$ , the function  $f(t + \tau(r))$  becomes almost independent of  $r$  at sufficiently late time,  $t \gg \tau(R)$ . The line vortex shape,  $v_\phi \approx f(t)/r$ , thus spreads out from the central region of the vortex with a time-dependent circulation “constant”  $C \approx f(t)$ . As time goes by (see fig. 23.4), the initial velocity profile is probed to farther and farther distances, again as a consequence of the monotonicity of  $\tau(r)$ . A steady vortex is, however, never reached unless the initial field,  $rv_\phi(r, 0) = f(\tau(r))$ , itself approaches a constant for  $r \rightarrow \infty$ .

These arguments show that it is in fact impossible to spin up a truly steady vortex by means of steady radial inflow, for the simple reason that it requires infinite angular momentum to be present in the flow to begin with. If the angular momentum is initially finite, all of it will sooner or later go down the drain, in agreement with common experience.

The process of getting out of a real bathtub cannot avoid leaving a certain amount of angular momentum in the water. It is this angular momentum that the inflow picks up and sends down the drain as a spinning vortex while the bathtub is being emptied (see problem 23.12). A real bathtub vortex may change speed and even stop up and reverse its sense of rotation depending on the details of how you got out of the water. In a bathtub of ordinary size the incidental initial angular momentum distribution is normally much greater than what can be provided by the slowly rotating Earth. The question of the Earth’s influence on the sense of rotation of a real bathtub vortex will be discussed in section 20.6.



## \* 23.5 Bathtub-like vortices

A bathtub vortex is an isolated liquid vortex with an open surface, sustained by radial inflow and powered by gravity. The most conspicuous feature of such a vortex is the central depression which may even penetrate the drain and make audible sounds. In the laboratory such vortices can be created in rotating containers (see section 20.5), but in this section we shall ignore the complication of container rotation and simply assume that the primary flow in the vortex is infinitely extended with the shape of a line vortex,  $rv_\phi \rightarrow C$ , at large distances. This guarantees an unlimited supply of mass and angular momentum, such that the vortex may be truly steady and not disappear down the drain as in real bathtubs<sup>2</sup>.

*Bathtub-like liquid vortex with open surface. At  $z = 0$  there is a drain-hole of radius  $a$ , and the “tub” has essentially infinite extension in the radial direction. There is a central depression of height  $h_0$  and the asymptotic liquid level is  $z = L$ .*

### Vortex equations

In a flat-Earth coordinate system with gravity as usual directed towards negative  $z$ , the vortex is drained through a circular hole of radius  $r = a$  situated at  $z = 0$ . The open liquid surface of the vortex is assumed to be rotationally invariant,  $z = h(r)$ . We shall again assume that the primary flow is cylindrical,  $v_\phi = v_\phi(r)$ , and it follows as before that the flow must obey the azimuthal equation (23-8), and that the radial flow is cylindrical,  $v_r = v_r(r)$ . Mass conservation again leads to an axial flow of the form (23-10).

Near the bottom of the container the cylindrical assumption must necessarily fail because of the no-slip boundary condition which requires the horizontal velocity to vanish right at the bottom of the container. This leads to the formation of a thin boundary layer (see section 20.4) that is not only capable of transporting fluid inwards but also deflects it upwards. In this sense, the boundary layer makes the bottom of the container appear as another source of fluid contributing to the radial inflow that drives the vortex. The actual upflow  $w(r)$  is determined by the properties of the bottom layer, but calculating the upflow requires the simultaneous solution of the coupled equations for the boundary layer and the bulk flow, and that leads to a rather complicated formalism [56].

### Nearly hydrostatic balance

If the secondary flow in the vortex is “sufficiently small”, the pressure gradient will as in hydrostatics be the only term in the Navier-Stokes equations that can balance gravity and deliver the centripetal force necessary for the circulating flow (see problem 23.5). Gravity makes the pressure  $z$ -dependent in addition to the  $r$ -dependence dictated by the centripetal forces required by the azimuthal flow. The equations of (nearly) hydrostatic balance are,

$$\frac{\partial p}{\partial z} = -\rho_0 g_0, \quad \frac{\partial p}{\partial r} = \rho_0 \frac{v_\phi^2}{r}. \quad (23-21)$$

<sup>2</sup>The following analysis is in part inspired by T. S. Lundgren, *The vortical flow above the drain-hole in a rotating vessel*, J. Fluid Mech. **155**, 381 (1985).

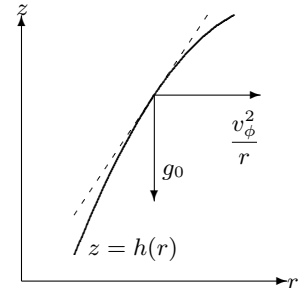
Using that the pressure is constant  $p = p_0$  at the open surface  $z = h(r)$ , it follows from first of these equations that

$$p(r, z) = p_0 + \rho_0 g_0 (h(r) - z) , \tag{23-22}$$

and inserting this into the second equation above we find,

$$\boxed{\frac{dh}{dr} = \frac{v_\phi^2}{g_0 r}} . \tag{23-23}$$

A simple geometrical construction reveals the meaning of this equation: the tangential component of gravity balances the tangential component of the centrifugal force at the rotating surface. Although a fluid particle sitting on the rotating surface feels no resulting tangential force from gravity and the centrifugal force, this does not mean that it necessarily sits still or moves with constant velocity, because inertial and viscous forces due to the secondary flow are also at play.



*A fluid particle sitting on the rotating surface of the vortex is subject to gravity and centrifugal force. The projections of these forces on the surface tangent (dashed) cancel in the leading approximation.*

The conditions for this equation to be valid are that the Reynolds number for the azimuthal flow is large,  $\text{Re}_\phi = r |v_\phi| / \nu \gg 1$ , that the radial flow is small compared with the azimuthal flow,  $|v_r| \ll |v_\phi|$ , and that the axial flow is small compared to the free fall velocity from the height  $h$ ,  $|v_z| \ll \sqrt{2g_0 h}$ . Torricelli's law (15-20) indicates that in the drain itself the vertical velocity will in fact be comparable to the free-fall velocity, so the last of these conditions can only be fulfilled far above the drain-hole. Since the pressure must in fact vanish at the open drain hole (for  $z = 0$  and  $r < a$ ), the derived form of the pressure (23-22) can simply not be right there. We shall not go further into these questions.

As  $rv_\phi \rightarrow C$  for  $r \rightarrow \infty$ , it follows from (23-23) that the liquid level of the asymptotic vortex is flat,  $h(r) \rightarrow L$  for  $r \rightarrow \infty$ . For the interpolating vortex (23-4), we may explicitly integrate (23-23) from  $r = 0$  to  $\infty$  to get the magnitude of the central depression,

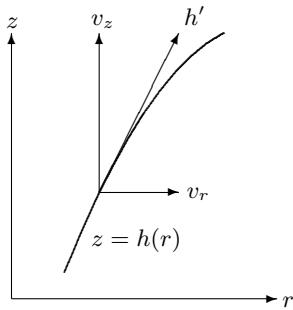
$$L - h_0 = \frac{1}{g_0} \int_0^\infty \frac{v_\phi(s)^2}{s} ds = k \frac{\Omega^2 c^2}{g_0} = k \frac{C^2}{g_0 c^2} , \tag{23-24}$$

where the coefficient,

$$k = \int_0^\infty \frac{(1 - e^{-s^2})^2}{s^3} ds = 0.693147 \dots , \tag{23-25}$$

is calculated by numeric integration.

**Example 23.5.1:** An interpolating vortex with core has radius  $c = 1$  cm, rotating 10 times a second, corresponding to  $\Omega = 63 \text{ s}^{-1}$ . The central depression becomes  $L - h_0 = 2.8$  cm.



The flowlines must have the same slope  $h' = dh/dr$  as the free surface.

### Surface flow condition

The existence of an open liquid surface with a depression at the center forces the inflow into a narrower region and thereby speeds it up in comparison with the simple axial jet of a tornado-like vortex. Consequently, there must exist a relation between the height of the surface,  $h(r)$ , and the radial inflow  $v_r(r)$ . The quantitative form of this relation is derived from the fact that the flowlines must follow the surface, or

$$v_z(r, h(r)) = v_r(r) \frac{dh(r)}{dr} \quad (23-26)$$

Putting  $z = h$  in (23-10), the resulting equation may be written,

$$\boxed{\frac{1}{r} \frac{d(rv_r h)}{dr} = w} \quad (23-27)$$

This provides the sought for relation between the radial flow and vortex shape.

Given the drain-flow  $w(r)$ , the three coupled ordinary differential equations (23-8), (23-27), and (23-23) determine the unknown functions,  $v_\phi$ ,  $v_r$  and  $h$ . They can in general only be solved by numerical methods.

### Plug-flow

The very simplest model is a pure “plug-flow” with a constant downflow  $-W$  inside the drain and vanishing upflow outside,

$$w = \begin{cases} -W & r < a \\ 0 & r > a \end{cases} \quad (23-28)$$

There is an unphysical jump in stress at the edge of the drain, which can be avoided using a softer drain-flow model.

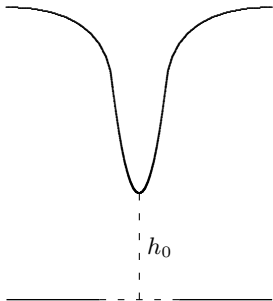
The axial flow could, for example, be controlled by a suction device removing liquid through the drain at a constant volume rate  $Q = \pi a^2 W$ . Alternatively, if gravity is the draining force, the velocity may in the nearly ideal case be estimated from Torricelli’s law (15-20),

$$W \approx \sqrt{2g_0 h_0}, \quad (23-29)$$

which is the free-fall velocity from the center of the surface depression.

The corresponding radial flow is calculated from (23-27) and becomes

$$v_r = -\frac{W}{2h(r)} \begin{cases} r & r < a \\ \frac{a^2}{r} & r > a \end{cases} \quad (23-30)$$



Torricelli’s law applied to the central streamline leads to  $W = \sqrt{2g_0 h_0}$  for a gravity-driven vortex.

For large  $r$ , the liquid surface is flat,  $h(r) = L + \mathcal{O}(r^{-2})$ , and the radial flow becomes that of a singular axial jet (23-14) with inflow parameter,

$$q = \frac{Wa^2}{2L}. \quad (23-31)$$

As before, we conclude that the asymptotic azimuthal flow is a line vortex for  $\text{Re}_r = q/\nu > 2$ . For  $r \rightarrow 0$ , the bottom of the dip is also flat,  $h(r) = h_0 + \mathcal{O}(r^2)$ , making the radial flow linear in  $r$  as in the Burgers vortex (23-13). In a vortex with a deep depression, the nonlinear correction terms to  $h(r)$  grow very fast with  $r$ , quickly making the linear approximation  $v_r \sim r$  invalid.

**Example 23.5.2:** A bathtub is filled with water to a height  $L = 50$  cm. When the plug (of radius  $a = 3$  cm) is pulled from the drain, the water falls freely through the drain with a velocity that maximally can be  $W \approx \sqrt{2g_0L} \approx 3.1 \text{ m s}^{-1}$ . The maximal asymptotic inflow parameter becomes  $q \approx 28 \text{ cm}^2/\text{s}$ , and since  $\nu = 8.6 \times 10^{-3} \text{ cm}^2/\text{s}$ , we find  $\text{Re}_r = q/\nu \approx 3200$ . The vertical Reynolds number,  $\text{Re}_z = 2Wa/\nu \approx 2 \times 10^5$ , is so large that we are probably not justified in using the present laminar theory.

### The depth of the depression

The core radius may be estimated from the condition that the radial Reynolds number passes through the value 2, as was the case for the Burgers vortex (23-13). Setting  $\text{Re}_r = r|v_r|/\nu \approx 2$  for  $r = c$ , we find from the inner solution in (23-30) that

$$c \approx \sqrt{\frac{4\nu h_c}{W}}, \quad (23-32)$$

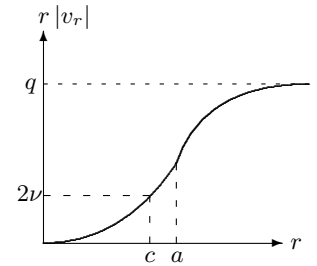
where  $h_c = h(c)$  is the height at the edge of the core. Since  $c/a = \sqrt{4\nu h_c/Wa^2} = \sqrt{2\nu/q \cdot h_c/L}$ , and since both factors inside the squareroot are smaller than unity, it follows that  $c < a$ . Thus it is consistent to use the inner solution, and the core lies normally entirely inside the drain.

To estimate the height of the vortex at the edge of the core, we use the interpolating vortex, in which it is roughly midway between the central and asymptotic heights,  $h_c \approx (L + h_0)/2$ . Likewise approximating the central depression with that of the interpolating vortex (23-24), we get the following equation,

$$L - h_0 = k \frac{C^2}{g_0} \frac{W}{2\nu(L + h_0)} \quad (23-33)$$

with  $k \approx 0.7$ . Solving for  $h_0$ , we finally obtain

$$h_0 \approx \sqrt{L^2 - k \frac{C^2 W}{2g_0 \nu}}. \quad (23-34)$$



The core radius is defined as the point where  $r|v_r|$  crosses  $2\nu$ . The core lies entirely inside the drain,  $c < a$ .

If the argument of the squareroot becomes negative, there is no solution because the central dip in the surface has plunged right through the drain, thereby violating the basic assumptions behind the model. We shall now verify that this estimate is reasonably precise.

### Numeric integration

The numeric integration of the coupled differential equations is sufficiently tricky to warrant a closer look. The many parameters make the problem somewhat confusing, but as we shall now see, there is in fact only two dimensionless scales in the problem.

First we rescale all variables to make them dimensionless,

$$\xi = \frac{r^2}{a^2}, \quad (23-35a)$$

$$w(r) = -Wf(\xi), \quad (23-35b)$$

$$h(r) = Lg(\xi), \quad (23-35c)$$

$$rv_\phi(r) = Cu(\xi), \quad (23-35d)$$

$$rv_r(r)h(r) = -\frac{1}{2}Wa^2v(\xi). \quad (23-35e)$$

In this parameterization, the coupled equations now take the form

$$v' = f, \quad (23-36a)$$

$$u'' = -\alpha u' \frac{v}{\xi g}, \quad (23-36b)$$

$$g' = \beta^2 \frac{u^2}{\xi^2}, \quad (23-36c)$$

with a prime denoting the derivative after  $\xi$ . All the confusing parameters have now been collected into only two  $\xi$ -independent “constants”,

$$\alpha = \frac{q}{2\nu} = \frac{Wa^2}{4L\nu}, \quad \beta = \frac{C}{a\sqrt{2g_0L}}, \quad (23-37)$$

and should be viewed as dimensionless measures of the strength of the asymptotic radial inflow  $rv_r \approx -q = -Wa^2/2L$  and the asymptotic circulation  $rv_\phi \approx C$ .

The estimate of the central height (23-34) becomes in the new variables

$$g(0) \approx \sqrt{1 - 4k\alpha\beta^2}. \quad (23-38)$$

The envelope of non-plunging central depressions is thus given by  $4k\alpha\beta^2 \lesssim 1$ , but one should remember that this inequality is based on rather coarse estimates and should not be expected to be exactly fulfilled.

The dimensionless functions,  $u$ ,  $v$ , and  $g$  are all required to approach unity for  $\xi \rightarrow \infty$ . The dimensionless drain-function  $f$  may in principle be freely chosen,



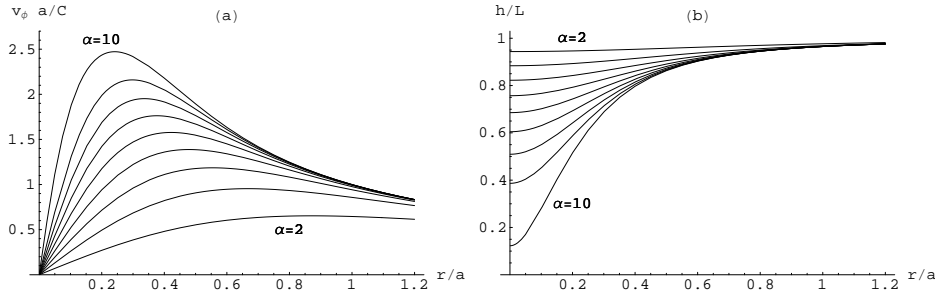


Figure 23.5: Azimuthal flow (left) and surface depression (right) for  $\beta = 0.188$  and  $\alpha = 2, 3, \dots, 10$ . The core radius corresponds roughly to the top in  $v_\phi$  and shrinks with growing secondary flow ( $\alpha$ ) whereas the depression deepens.

but we shall for numerical convenience choose it to be a soft plug-flow of the form,

$$f(\xi) = e^{-\xi} , \quad (23-39)$$

rather than the step function that corresponds to discontinuous plug-flow (23-28). With this choice eq. (23-36a) may be explicitly solved, using the boundary condition that  $v(\infty) = 1$ , with the result

$$v(\xi) = 1 - e^{-\xi} . \quad (23-40)$$

This reduces the number of coupled differential equations (23-36) to two.

The coupled equations are solved by imposing boundary conditions at  $\xi = 0$  where  $u(0) = 0$ ,  $u'(0) = s$ ,  $v(0) = 0$ , and  $g(0) = m$ . Starting with some choice of  $s$  and  $m$ , a search is made for those values that lead to fulfillment of the boundary conditions at infinity,  $u(\infty) = v(\infty) = g(\infty) = 1$ . For the soft plug-flow model, the result is shown in fig. 23.5 for the particular value  $\beta = 0.188$ , which allows for a maximal value of  $\alpha = 10$ . The corresponding envelope parameter becomes  $4k\alpha\beta^2 = 0.99$ , and the estimated central height  $h_0/L = 0.1$ . Generally, the envelope to non-plunging behavior is determined by the appearance of numerical instabilities, and the envelope is found to be very close to the estimate  $4k\alpha\beta^2 \approx 1$  for all  $\beta$  and  $\alpha \gtrsim 2$ .

## Problems

**23.1** Show that the vertical vorticity in the Rankine vortex is

$$\omega_z = \begin{cases} 2\Omega & r < a \\ 0 & r > a \end{cases} \quad (23-41)$$

**23.2** Calculate the kinetic energy of the Rankine vortex inside a radial distance  $r \leq R$  and axial length  $L$ .

**23.3** Show that the circulation around a Rankine vortex is independent of the curve, as long as it encircles the axis of the vortex and lies entirely outside the core.

**23.4** a) Calculate the effective pressure a Rankine vortex. b) Find the surface shape of a liquid Rankine vortex in constant gravity. c) What is the depth of the depression. d) Calculate the depth for a Rankine vortex with core radius  $c = 1$  cm, rotating 10 times a second.

**23.5** Assume that the velocity fields  $v_{r,\phi,z}$  in cylindrical coordinates only depend on  $r$  and  $z$ . Show that the Navier-Stokes equations become

$$\frac{\partial v_\phi}{\partial t} + v_r \frac{\partial v_\phi}{\partial r} + \frac{v_r v_\phi}{r} + v_z \frac{\partial v_\phi}{\partial z} = \nu \left( \frac{\partial^2 v_\phi}{\partial r^2} + \frac{1}{r} \frac{\partial v_\phi}{\partial r} - \frac{v_\phi}{r^2} + \frac{\partial^2 v_\phi}{\partial z^2} \right), \quad (23-42a)$$

$$\frac{\partial v_r}{\partial t} + v_r \frac{\partial v_r}{\partial r} - \frac{v_\phi^2}{r} + v_z \frac{\partial v_r}{\partial z} = \nu \left( \frac{\partial^2 v_r}{\partial r^2} + \frac{1}{r} \frac{\partial v_r}{\partial r} - \frac{v_r}{r^2} + \frac{\partial^2 v_r}{\partial z^2} \right) - \frac{1}{\rho_0} \frac{\partial p^*}{\partial r}, \quad (23-42b)$$

$$\frac{\partial v_z}{\partial t} + v_r \frac{\partial v_z}{\partial r} + v_z \frac{\partial v_z}{\partial z} = \nu \left( \frac{\partial^2 v_z}{\partial r^2} + \frac{1}{r} \frac{\partial v_z}{\partial r} + \frac{\partial^2 v_z}{\partial z^2} \right) - \frac{1}{\rho_0} \frac{\partial p^*}{\partial z}, \quad (23-42c)$$

with the incompressibility condition

$$\frac{\partial v_r}{\partial r} + \frac{v_r}{r} + \frac{\partial v_z}{\partial z} = 0 \quad (23-43)$$

**23.6** Calculate the streamlines for the Burgers vortex.

**23.7** Calculate the exact pressure for the Burgers vortex.

**23.8** a) Show that the so-called Taylor vortex

$$v_\phi(r, t) = \tau \frac{r}{t^2} e^{-r^2/4\nu t}, \quad (23-44)$$

is a solution to (23-6) where  $\tau$  is a constant with dimension of time. b) Calculate the total angular momentum for a stretch of length  $L$  of the Taylor vortex and show that it is constant in time.

**23.9** Assume that a free cylindrical vortex only depends on the dimensionless variable

$$\xi = \frac{r^2}{4\nu t} . \quad (23-45)$$

and assume that

$$v_\phi(r, t) = \frac{F(t)}{r} f(\xi) , \quad (23-46)$$

where  $F(t)$  is a time-dependent factor.

- a) Find a differential equation for  $f(\xi)$ .
- b) Show that  $F(t) \sim t^{-\alpha}$  where  $\alpha$  is a dimensionless parameter.
- c) Show that the solution is

$$f_\alpha(\xi) = \sum_{n=0}^{\infty} \frac{(n + \alpha)!}{n! \alpha!} (-1)^n \frac{\xi^{n+1}}{(n + 1)!} \quad (23-47)$$

- d) Find a closed form for  $\alpha = 0, 1, 2$  and draw the vortex shapes.

**23.10** Show explicitly that the interpolating field (23-4) together with the Burgers secondary flow (23-13) is a solution to the Navier-Stokes equations for steady incompressible fluid, (17-17) and (18-2).

**23.11** Assume that a vortex at  $t = 0$  has the shape of an interpolating vortex (23-4) with radius  $b$ , and that there is a radial inflow identical to that of the Burgers vortex (23-13) corresponding to a radius  $a$ . Determine how the azimuthal flow of the original vortex converges upon the interpolating function of radius  $a$ .

**23.12** Assume that the water in a bathtub originally rotates like a solid body,  $v_\phi = \Omega r$ , far from the drain. Determine the far field at a later time and the rate at which angular momentum flows in towards the drain.

**23.13** Show that the vortex equation (23-8) may be solved explicitly by quadrature when  $v_r(r)$  is given.

**23.14** a) Show that the divergence condition can be solved by means of a field  $\psi(r, z)$  (a stream function) satisfying

$$\frac{\partial \psi}{\partial z} = r v_r , \quad \frac{\partial \psi}{\partial r} = -r v_z \quad (23-48)$$

- b) Show that the streamlines satisfy

$$\psi(r, z) = \text{const} \quad (23-49)$$

- c) Show that the stream function for a cylindrically invariant vortex is

$$\psi(r, z) = r v_r(r) z - \int r w(r) dr \quad (23-50)$$

and use this result to find the streamlines for the various cylindrically invariant vortices.

**23.15** Consider a tornado-like vortex plug-flow and constant  $h(r) = L$ . Show that the vortex theory of section 23.5 leads to a solution

$$v_\phi = \begin{cases} \frac{\Omega c^2}{r} \left(1 - e^{-r^2/c^2}\right), & (r < a) \\ \frac{\Omega c^2}{r} \left(1 + \frac{e^{-\alpha}}{\alpha-1} \left(1 - \alpha \left(\frac{a^2}{r^2}\right)^{\alpha-1}\right)\right), & (r > a) \end{cases}. \quad (23-51)$$

where  $\Omega$  is the angular velocity of the core and

$$c = \frac{a}{\sqrt{\alpha}}. \quad (23-52)$$

is the core radius.